



## Shaping of amplified beam from a highly multimode Yb-doped fiber using transmission matrix

Raphaël Florentin, Vincent Kermène, Agnès Desfarges-Berthelemot, Alain  
Barthélémy

### ► To cite this version:

Raphaël Florentin, Vincent Kermène, Agnès Desfarges-Berthelemot, Alain Barthélémy. Shaping of amplified beam from a highly multimode Yb-doped fiber using transmission matrix. *Optics Express*, 2019, 27 (22), pp.32638. 10.1364/OE.27.032638 . hal-02384298

**HAL Id: hal-02384298**

**<https://hal.science/hal-02384298>**

Submitted on 30 Nov 2020

**HAL** is a multi-disciplinary open access archive for the deposit and dissemination of scientific research documents, whether they are published or not. The documents may come from teaching and research institutions in France or abroad, or from public or private research centers.

L'archive ouverte pluridisciplinaire **HAL**, est destinée au dépôt et à la diffusion de documents scientifiques de niveau recherche, publiés ou non, émanant des établissements d'enseignement et de recherche français ou étrangers, des laboratoires publics ou privés.



# Shaping of amplified beam from a highly multimode Yb-doped fiber using transmission matrix

RAPHAEL FLORENTIN, VINCENT KERMENE, AGNÈS DESFARGES-BERTHELENOT,\* AND ALAIN BARTHELEMY

Université de Limoges, CNRS, XLIM, UMR 7252, 123 Avenue Albert Thomas, F-87000 Limoges, France

\*agnes.desfarges-berthelenot@xlim.fr

**Abstract:** The transmission matrix of an ytterbium doped multimode fiber with gain was measured. It was shown to vary owing to the pump power level. Amplified beam focusing, beam steering and shaping were demonstrated using the measured matrix for input wavefront shaping, with an efficiency similar to the case of a passive fiber. The impact of weak gain saturation was lastly investigated.

© 2019 Optical Society of America under the terms of the [OSA Open Access Publishing Agreement](#)

## 1. Introduction

Multimode fibers (MMF) share some analogies with the disordered media, because of mode coupling which scatters light fields among the different guided modes [1]. Coupling may occur spontaneously because of fiber imperfections or it can be made by applied stress and bending [2]. So, these last years, MMF were used as a convenient experimental platform for investigations on light transport in complex media [3,4,5,6]. Pioneering works showed that the spatial pattern of a laser beam transmitted by a scattering media can be controlled by shaping the wavefront of the input signal [7]. Multiple wave interferences in the output plane were adjusted through a transverse phase modulation of the input determined by an optimization loop. The approach was next adapted to multimode fibers [8], to prevent from laser beam quality degradation but also to focus and steer the delivered output beam. Since then, many other techniques have appeared to circumvent the complex random transformation suffered by light waves during their travel through a MMF. They rely for instance on digital optical phase conjugation [9], or on transmission matrix (TM) measurement [10] or on deep learning [11] or on correlations [12]. Beyond the optical communication domain, multimode fibers have been used for a broad range of applications including flexible imaging [13], optical tweezers [8,14], 3D microfabrication [15] or remote image classification and recognition [16], spectroscopy [17], quantum processing [18], etc. Most if not all the above mentioned techniques and applications have considered passive multimode fibers only.

Very few studies dealt with light beam control in MMF with gain or loss [6,19,20]. Amplification together with selection of the sole fundamental mode has been achieved in the past by various means like mode dependent gain, provided by optimization of the doped cross-section, or mode dependent losses through fiber coiling [21,22]. Later on, most of the research has been directed towards the design and fabrication of large mode area single mode fibers for high power laser amplification [23]. However, MMF amplifiers are requested for spatial division multiplexing (SDM) in optical communications. For laser power amplifier they could be a good alternative to large mode area fibers because of their lower cost technology and higher flexibility. In addition MMF amplifier combined with active input control could offer supplementary functionalities without the addition of distal device. Considering few mode Erbium doped fibers [24], wavefront tailoring of the input signal served for modal gain equalization, a crucial issue for SDM communications. Rare-earth doped fibers propagating a large number of modes could be

of interest in the manufacturing industry to realize smart amplifying system which could directly deliver high power complex beam pattern on demand. For that purpose, laser beam shaping by an iterative adaptive control of the input wavefront feeding an amplifying multimode fiber was demonstrated to be a potential option [25]. In this article, we show that laser beam focusing and shaping through an amplifying multimode fiber can also be efficiently achieved by measuring its TM under pumping. The benefit is that a single measurement of the TM suffices to achieve any desired output pattern.

In the following sections, we report the TM measurement of a highly multimode fiber with gain for the first time, using the co-propagative reference scheme [26,27]. TM was further used for input wavefront profiling to get output beam focusing and shaping in amplification regime. Intensity enhancement of the shaped foci was investigated. Transmission matrices are relevant when the system under concern behaves in a linear way. This holds true even in the case of a dissipative system exhibiting loss or gain. In the case of a medium with gain however, linearity is restricted to the so called small signal gain regime. In such a case, the upper state of the active ions stays strongly populated with respect to the ground state of the transition and the signal input power remains well below the saturation power. The shaping capabilities offered by the TM were assessed here in the linear gain regime but also in the early stage of the gain saturation regime.

## 2. TM measurement

For TM measurement, one needs to choose input and output bases for the optical field expansion and most importantly to access the complex amplitude of the fiber output field, connected to each excitation of the input basis. In our case, the input basis was based either on tilted plane waves (sampling of the transverse wave vector space) or on random phase profiles. The output basis corresponded to the pixels of a camera (the canonical basis) which imaged the output facet of the multimode fiber, as usually done. Different strategies can be followed to measure the fiber output transverse field in order to derive the complex valued coefficients of the multimode fiber TM. It can be based on interference with a reference beam [28], on phase retrieval techniques [29] or on amplitude correlations by diffraction on computer generated holograms [10]. In addition to mode dependent propagation constant and to mode coupling which govern coherent light transmission through passive fiber, in active fibers there is also the potential impact of mode dependent gain and the effect of the thermal load, due to the pumping at high power and to non-radiative energy transfer of the excited ions. Amplified spontaneous emission may also degrade the signal to noise ratio in the amplified beam. Thermal effects in particular, strongly vary the mode propagation constant and they may change as well the input coupling conditions. This results in drift in the experimental settings and in the fiber properties (phase and group delays) when the pump level is set on and also each time a thermal equilibrium is not reached. These parameters brings extra difficulties to the measurement of TM of a medium with gain which might explain why it was not previously done. To circumvent some of the above mentioned issues in the measurement of the gain fiber TM we chose a scheme with a co-propagative reference. This configuration mitigates the differential phase drift between signal and reference fields on the duration of the measurement as they share the same propagation medium. The TM measurement technique is similar to the one previously described in [27]. Figure 1 shows the experimental setup. A linearly polarized Gaussian laser beam delivered by a CW fibered laser source at 1064 nm is collimated and magnified by a telescope to cover the surface of a fast Segmented Deformable Mirror (SDM) made of 952 actuators (KiloDM, Boston Micromachines). Only a few pixels (5%) of the SDM, randomly distributed, generate the reference beam by wavefront division. The 900 remaining pixels serve to shape the transverse wavefront according to the input basis elements. The beam shaped by the SDM is subsequently down sized by a couple of telescopes and launched in the multimode fiber. The active multimode fiber is a double clad step index fiber from Nufern with about 104 LP guided modes per polarization. Its core is 90 $\mu$ m in diameter with

a numerical aperture (NA) of 0.10. A 450 $\mu$ m pump cladding diameter of 0.24 NA surrounds the Ytterbium doped fiber core. A multimode pump beam, from a fiber coupled CW laser diode at 976 nm (Lumics LuOcean P2 LU0976C), is launched into the fiber clad through a dichroic beam splitter (DBS) in a backward propagating scheme with respect to the signal wave. The 1.5 m long Yb:MMF is freely coiled on the table with a minimum curvature radius of 15 cm. On the opposite end, the fiber output field is imaged on a high dynamic CCD camera (FLIR Grasshopper 3), in such a way to cover a reduced sensor area of  $M = 128 \times 128$  pixels.

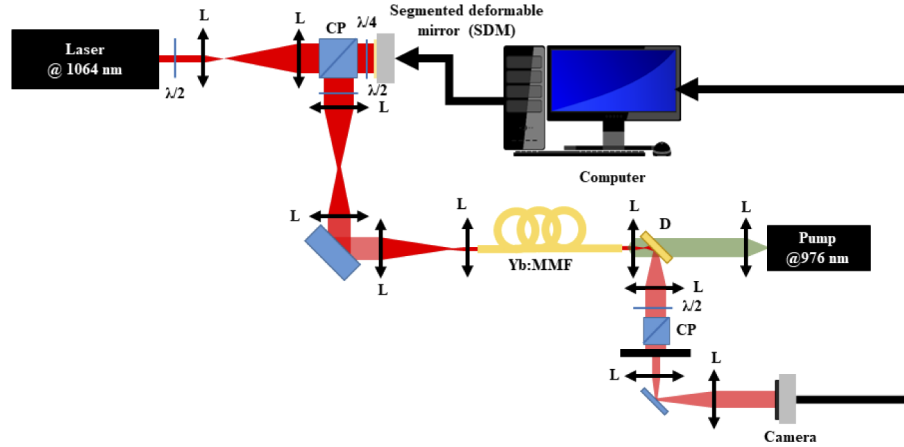


**Fig. 1.** Experimental set-up for the measurement of the transmission matrix of the Yb:MMF with gain

The rectangular TM has thus the following dimensions  $N \times M = 900 \times 16,384$ . A phase stepping interferometry technique is used to retrieve the phase of the corresponding output fields with respect to the co-propagative reference. The TM measured in this way is not the real matrix because the reference field at the output of the fiber is not uniform. In fact we measured  $TM = TM_{\text{real}} \times RM$  (element wise product), where RM is a matrix whose lines are identical and represents the complex amplitudes of the fixed reference, that remains unknown here. However, as long as the reference beam does not change, it is possible to shape the signal at the fiber output (focusing, imaging), using the measured TM. Provided that a normalization is made, the measured TM displays as well the same statistical properties, approximately, as the actual TM [26]. This TM is built in less than 1 minute from the  $4 \times N$  recorded images provided by the 4-states phase stepping interferometry process. After preliminary adjustment, we performed TM measurements with the pump in off state (passive fiber) and then set on (fiber with gain) at various power level between (5 to 20 W) to change the overall gain (2.3 to 21 dB). The TM clearly evolved with gain.

### 3. Beam focusing and amplification

A first assessment of the recorded  $TM$  is given by its use for output signal focusing. The input beam must be shaped according to the phase profile given by the elements of one line of the  $TM^\dagger$  (where dag stands for conjugate transpose). The line index is directly connected to the transverse position of the desired focus on the fiber output facet. Based on the measured matrices one can therefore compute the so called focusing operator [26] (or the time reversal operator) given by:

$$O_{\text{foc}} = TM \cdot TM_{\text{norm}}^\dagger \quad (1)$$

where the elements of  $TM_{\text{norm}}$  have been normalized to their modulus,  $\frac{a_{ij}}{|a_{ij}|}$ , to take into account the phase-only shaping of the fiber excitation. The diagonal of  $O_{\text{foc}}$  denotes the focusing efficiency

which could be achieved in practice on the whole fiber cross section. Figure 2 reports the focusing efficiency pattern computed from the TM measured for a gain of 13.5 dB. The pattern is quite similar to the case of a passive fiber and shows that a focus of amplified light may be formed almost anywhere across the fiber core. A few dark points in Fig. 2 indicate however a local drop in efficiency which could be connected with the use of a speckled reference wave.

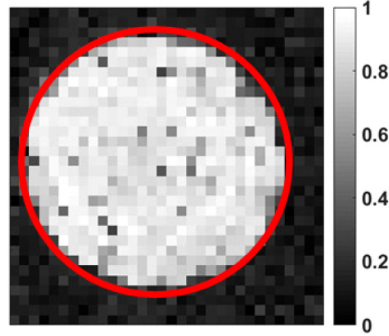


**Fig. 2.** Map of the focusing efficiency normalized to its peak value on the output fiber cross-section. Values derive from the focusing operator of the measured transmission matrix at 13.5 dB gain.

Based on the measured matrices, the wavefront shaping system described Fig. 1 was used to focus the output signal in a sharp spot (about the same size as the average speckle grain generally observed at the fiber output:  $\lambda/2NA$ ) in various locations on the Yb:MMF core cross-section, both without and with gain. Some typical examples are presented in Fig. 3.

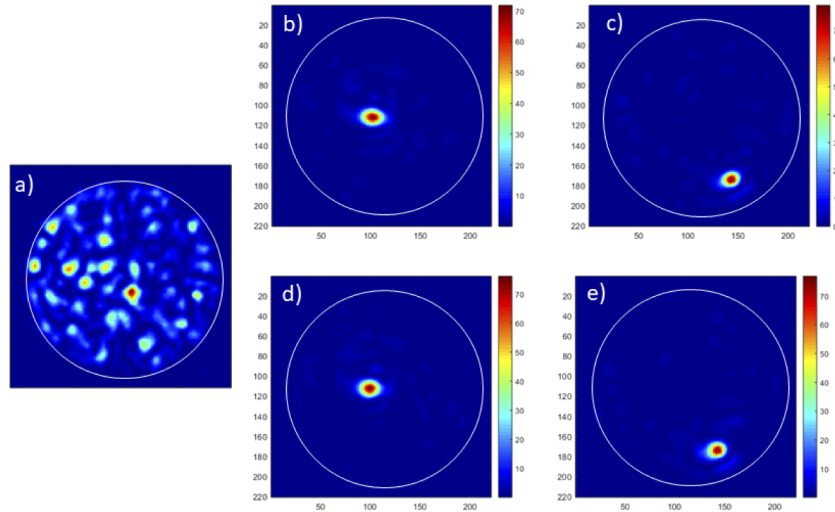


**Fig. 3.** Comparison between different intensity patterns at the MMF output observed for (a) a random input wavefront (b) and (c) for an input shaped for focusing in passive regime respectively close to center and close to the cladding, (d) and (e) for an input shaped for focusing respectively close to center and close to the cladding for a 10 dB gain.

As a standard feature, the intensity enhancement parameter  $\eta$  quantifies the focusing efficiency [30], defined as the ratio between the peak intensity  $\hat{I}$  of the focused beam and the average value of the background intensity  $\langle I \rangle$  on the whole core cross-section:  $\eta = \hat{I} / \langle I \rangle$ . Wherever the focusing

on the core cross-section and whatever the operating regime (without and with gain), the intensity enhancements were quite similar. In addition, the high level of the measured enhancement,  $\eta=72, 79, 76, 77$  respectively for Figs. 3(b), 3(c), 3(d) and 3(e), confirms the efficiency of the TM measurement for a complex medium with gain. For reference, the theoretical intensity enhancement for a phase only input shaping is given by  $\eta_{th} = \pi/4 \cdot (N-1) + 1$  [30] where  $N$  denotes the number of degrees of freedom of the whole device. Here the degrees of freedom are bounded by the number of fiber modes so that  $\eta_{th} = 82$ . Needless to say that with the measurement of a single TM it is therefore possible to raster scan a focused amplified beam at the fiber output with shaping of the input wavefront evolving overtime. The evolution of the intensity enhancement was recorded for various position of the focus on the fiber active core (see Fig. 4).

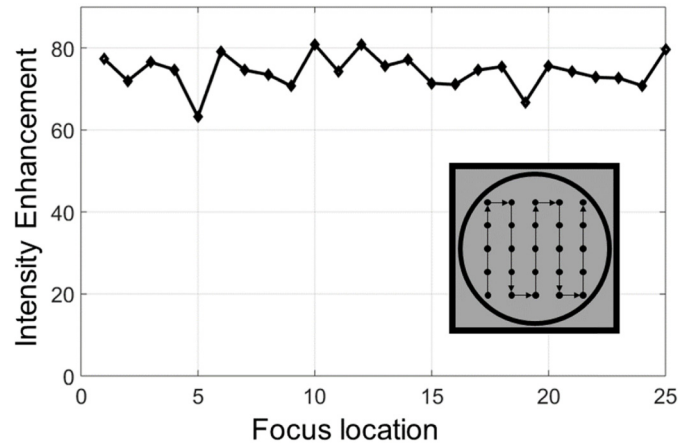


**Fig. 4.** Intensity enhancement of the focus measured at 13.5 dB gain for 25 different positions in the Yb:MMF core cross-section (as illustrated in the inset).

Data show weak fluctuations with peak values approaching the theoretical limit for focus close to the core boundary likely to be connected with the contribution of the modes of highest order. A fast ( $> 10$  kHz) raster scanning was realized at the Yb:MMF output thanks to the high actuation speed of the MEMS based segmented mirror used for shaping. Focusing and scanning at a distance from the fiber output facet can be done simply by considering free space propagation between the two planes through a propagation matrix  $P$ . Thus the new  $TM$  to consider for input shaping writes  $TM_P = P \cdot TM$  and does not need a new measurement. Amplified beam focusing has been achieved for various gain values. The signal input power was kept constant while the pump power was changed to modify the Yb:MMF gain (Fig. 5). Keeping fixed the input wavefront, the shaped focus vanished and beam control was lost after each change in pump power. To preserve output shaping capabilities it was mandatory to renew the TM measurement for the pump level under concern. This shows that the TM significantly evolved with pump power and gain. Several parameters can contribute to the evolution of the TMs such as thermal distortions or non-uniform modal gain or gain induced modal coupling. The focusing efficiency was observed to be similar to the passive case and to be almost independent of the gain level, as shown on Fig. 4, whereas the measured TM significantly changed. All the gain values given throughout the paper were based on output powers measured switching on and off the pump whilst keeping the input wavefront profile unchanged. This was done to exclude the variations in fiber coupling efficiency due to the wavefront shaping.

Similarly to the passive case, it was also possible to perform the simultaneous display of multiple foci, with a controlled phase relationship, by launching in the fiber a linear combination



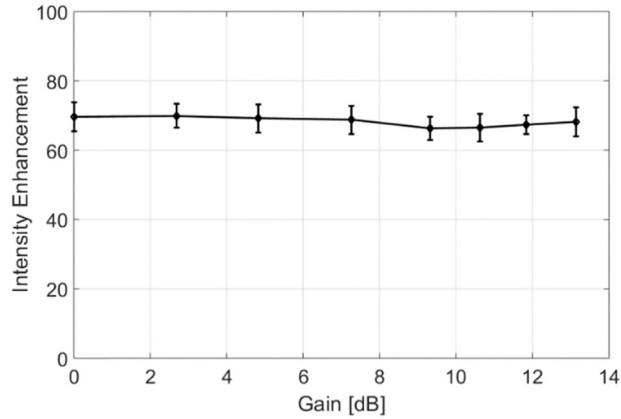


**Fig. 5.** Focusing enhancement parameter, average of 25 focusing on different positions in the MMF core cross-section, owing to the fiber amplification (input power = 20 mW). The line is a guide for the eye.

of their corresponding inputs according to the relationship.

$$E_{in} = \frac{TM^\dagger \cdot E_{out}}{|TM^\dagger \cdot E_{out}|} \quad (2)$$

Examples of shaping in two and three foci of balanced intensity are presented in Fig. 6 for a gain of 13.5 dB. The intensity enhancement on the shaped spots decreases as theoretically expected when their number grows.

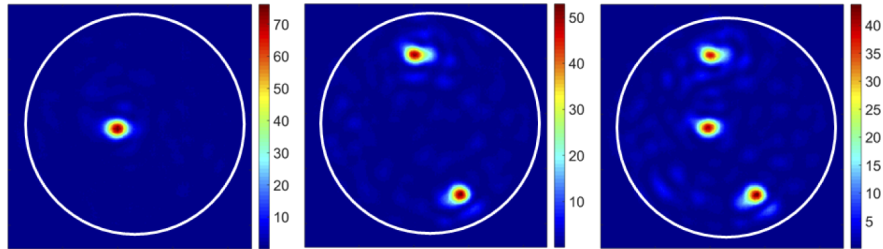


**Fig. 6.** Examples of simultaneous focusing on two and three light spots on the fiber output facet for a gain of 13.5 dB, together with the single focus case as reference.

#### 4. Gain saturation regime

In our experimental set-up, starting from a small signal gain of 13.5dB gain ( $P_{\text{pump}} \sim 16.5\text{W}$ ) we could decrease the gain down to 7.8 dB by raising the signal power launched into the fiber, from 4.9 mW to 486 mW, reaching a saturation level of almost - 6 dB. We investigated the impact of gain saturation on the beam control capability offered by transmission matrix at the active multimode fiber output. The nonlinearity due to gain saturation was expected to alter the shaping since the TM approach relies on a linear behavior of the whole set-up. Our aim was to determine how fast. In a first step, the transmission matrix measured in linear gain regime was used to get focusing of the amplified output. Then, keeping fixed the structuration of the input wave, we recorded the evolution of the output beam pattern while the gain was varied by increasing the signal power. The focus spot was preserved in presence of saturation even though a slight

deterioration of the spot shape was noticed. A stronger impact was measured on the intensity enhancement which slowly dropped from  $\sim 80$  down to  $\sim 56$  when the gain reduced progressively from 12.2 to 8.6 dB (see red line and inset in Fig. 7). The coupling conditions were kept constant, but saturation brought a signal power dependent complex 3D heterogeneity in the population level of the upper state of the emission transition of Yb ions and hence in the material response [31]. This may have changed the amplitude of the output modes whose interference gave rise to the beam focusing. Most importantly, gain-phase coupling, connected with Kramers-Kronig relationships, introduce a resonant nonlinear phase-shift which may vary from one mode to another [32]. We guess this was the major contribution to the saturation induced loss in shaping efficiency.

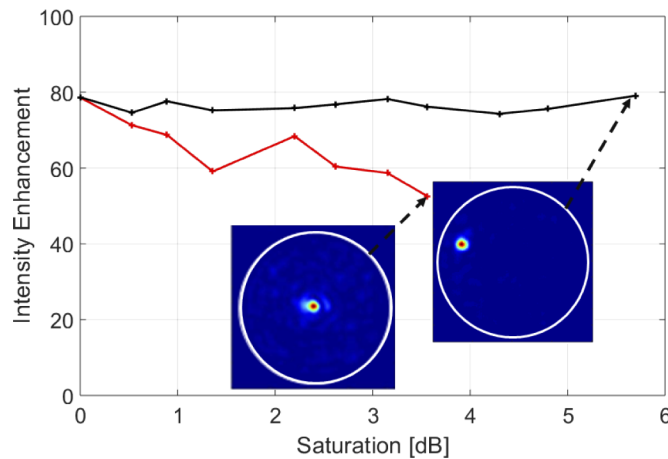


**Fig. 7.** In red: Enhancement parameter for a focus located close to the center of the MMF output facet, owing to the MMF gain which evolved by saturation because the signal input power was varied. A single TM was used for focusing which was measured in small signal gain condition. The input wavefront shaping was the same for each saturation level. An example of degraded focusing is given in inset In black: Intensity enhancement parameter for a focus, averaged on different positions, owing to the MMF gain which evolved by saturation because the signal input power was varied. Different TMs were used for focusing which were measured for each saturation condition. An example of focus image is given in inset.

In a second experiment, the transmission matrix was measured for every values of the input signal power, i.e. for different levels of gain saturation and subsequently used for focusing keeping the same signal level. The measurement technique itself being based on a linear response of the system under test, we expected that using the resulting TM to perform shaping should fail. On the contrary, beam focusing on the fiber output face was still achievable on the desired position (see inset of Fig. 7). The intensity enhancement even was preserved at the level which was observed in the passive and linear gain regimes (Fig. 7 in black). All happened as if the TM measured under saturation was not significantly spoiled by the nonlinearity due to the gain. However, we observed a deviation from a purely linear behavior when we used the measured TM for a more complex beam shaping which involved several rows of the TM. As an example the fiber output was shaped in a triplet of light spots (see right image of Fig. 6). The input wavefront was structured to get three foci of equal intensity according to Eq. 2.

The corresponding output images shown a deviation from the expected beam shaping in the saturated gain regime. Although it was possible to shape a triplet of output beams, their intensity was not identical as expected. It evolved owing to the gain regime and significantly departed from a uniform value (see Fig. 8). The observed beam intensity profile agreed with the desired



one for the small signal gain operation only (saturation  $< 1$  dB). This is a signature of nonlinearity although it is weak since the triple peak shape was preserved. The TMs approach was close to the boundaries of its validity domain in the investigated situation. However, in most of the amplifying regimes, at least with our experimental conditions (multiple Watts class Yb doped step index MMF), TMs can be measured and considered as a good description of the spatial transformations achieved by propagation and amplification in the Yb-MMF.

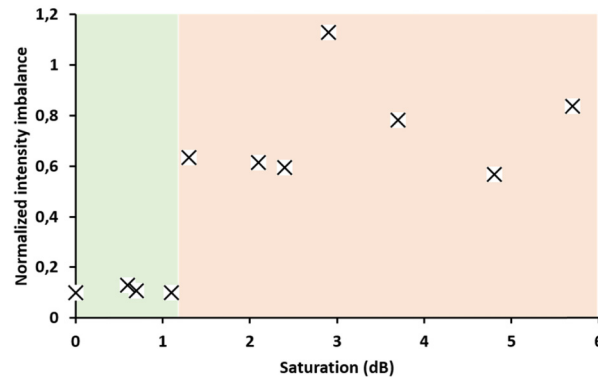


**Fig. 8.** Normalized peak to valley deviation in intensity enhancement among a spot triplet (right image of Fig. 6) versus gain saturation. An input wavefront structuration derived from the different TM measured for each level of gain saturation was applied to form three light spots of identical intensity. Above 1dB saturation the amplified beam control was degraded.

## 5. Transmission eigenchannels

Singular Value Decomposition (SVD) of the TMs was computed and we plotted the normalized singular values (SV) distributions (see Fig. 9). We can assume that the eigenchannels associated to the first hundred singular values are the actual transmission channels, since the maximum number of independent channels should be bounded by the maximum number of modes the Yb-MMF can guide. Indeed, with gain there is a noticeable change of slope in the SV distribution (in log scale) around eigenchannel number  $\sim 150$  which departs from the smooth evolution of the distribution corresponding to the passive case. That could identify the genuine number of freedom degree in the system.

Beyond that eigenchannel number, singular values and singular vectors are mostly impacted by detection noise and should not be considered as meaningful. The curves show that with or without gain, the first hundred singular values nearly follow the same evolution. Because of the measurement technique, where the reference is left undetermined, it is not possible to recover the TM in the MMF's mode basis from the measured TM. Therefore the TMs represent here the whole coherent optical field transformation between the DM and the output camera. So a possible explanation for the preservation of the SV distribution with gain could be that the most transmitted singular modes are governed by the MMF input coupling conditions and their associated losses. Turning the MMF from passive transmission to transmission with gain did not modify this spatial filtering but just provided uniform amplification to the singular modes with good coupling efficiency.

As an example of the complex shaping capability offered by the measured TM, a set of three output singular vectors is shown Fig. 10 corresponding to a 12.4 dB gain. The theoretical patterns are given by the SVD of the measured TM. The experimental patterns were recorded at the fiber output while the DM shaped the input according to the phase profile of the theoretical input singular vectors. The agreement between the theoretical and experimental images is rather good.

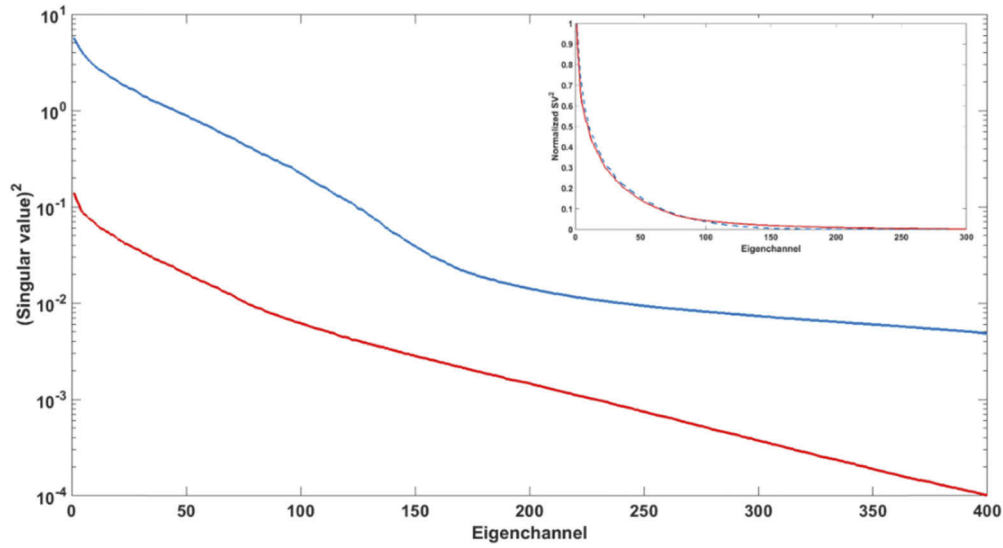


**Fig. 9.** Singular values (log scale) of the measured TM eigenchannels for the passive fiber (red), and for an amplifying fiber with 13.5 dB gain (blue). Traces have been normalized to the measured transmission for an excitation of the first transmission channel (singular vector). Squared singular values normalized to their peak value are given in a linear scale in the inset to highlight their similar distribution profile for the first hundred channels

It completes the demonstration of the shaping capabilities of the TM approach in a MMF with gain. From the TMs measured without and with gain, we obtained different singular vector transverse patterns for a fixed eigenchannel number. It confirms that TMs changed with the addition of gain as previously stated.

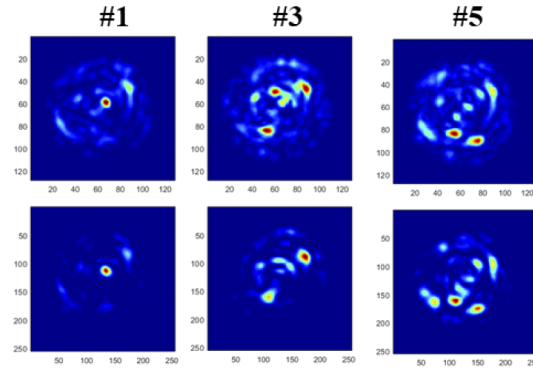


**Fig. 10.** Three of the first output singular vectors for a gain of 12.4 dB. Top line, patterns computed from the measured TM. Bottom line, patterns recorded at the fiber output after input shaping according to the theoretical input singular vectors.

## 6. Conclusion

We have carried out measurement of the transmission matrix of a step-index Yb-doped multimode fiber in amplification regime. The measurement technique, based on a co-propagative reference scheme, was not spoiled by the presence of gain. The TM evolved with gain but the stronger

impact might come from thermal effects related to the launched pump power which vary the mode propagation constants. Non uniform modal gain or gain induced coupling could be another source of alteration. The TM measured at a given gain level, was effective in focusing and shaping the transverse pattern of the amplified output. Beam focusing in particular gave the same intensity enhancement as in the passive case up to the maximum gain ( $\times 22.4$ ) and up to the maximum power (3W) we were able to realize in experiments. The profile of the distribution of SV of TM does not evolve with gain while the SV patterns depend on the gain level. The MMF amplifier output was shaped according to some of the TM's singular vector in good agreement with the expectations. The TM measured in small signal gain regime changed under gain saturation. This was expected because of the nonlinearity generated by saturation. But it was unexpected that the TM measured in saturation regime still permits to achieve focusing with almost no loss in intensity enhancement. Even for gain drop of  $\sim 6$ dB (the maximum we could reach in experiment) the nonlinearity might be too weak to significantly impact the TM measurement and to hinder the focusing. However deviation from a strict linearity was highlighted by a more complex multiple spot shaping.

## Funding

Agence Nationale de la Recherche.

## References

1. C. Antonelli, A. Mecozzi, M. Shtaif, and P. J. Winzer, "Random coupling between groups of degenerate fiber modes in mode multiplexed transmission," *Opt. Express* **21**(8), 9484–9490 (2013).
2. W. Xiong, P. Ambichl, Y. Bromberg, B. Redding, S. Rotter, and H. Cao, "Spatiotemporal control of light transmission through a multimode fiber with strong mode coupling," *Phys. Rev. Lett.* **117**(5), 053901 (2016).
3. S. Fan and J. M. Kahn, "Principal modes in multimode waveguides," *Opt. Lett.* **30**(2), 135–137 (2005).
4. J. Carpenter, B. J. Eggleton, and J. Schröder, "Observation of Eisenbud–Wigner–Smith states as principal modes in multimode fibre," *Nat. Photonics* **9**(11), 751–757 (2015).
5. P. Ambichl, W. Xiong, Y. Bromberg, B. Redding, H. Cao, and S. Rotter, "Super- and anti-principal-modes in multimode waveguides," *Phys. Rev. X* **7**(4), 041053 (2017).
6. P. Chiarawongse, H. Li, W. Xiong, C. W. Hsu, H. Cao, and T. Kottos, "Statistical description of light transport in multimode fibers with mode dependent loss," *New J. Phys.* **20**(11), 113028 (2018).
7. I. M. Vellekoop and A. P. Mosk, "Focusing coherent light through opaque strongly scattering media," *Opt. Lett.* **32**(16), 2309–2311 (2007).
8. R. Di Leonardo and S. Bianchi, "Hologram transmission through multi-mode optical fibers," *Opt. Express* **19**(1), 247–254 (2011).
9. I. N. Papadopoulos, S. Farahi, C. Moser, and D. Psaltis, "Focusing and scanning light through a multimode optical fiber using digital phase conjugation," *Opt. Express* **20**(10), 10583–10590 (2012).
10. J. Carpenter, B. J. Eggleton, and J. Schröder, "110 (110 optical mode transfer matrix inversion)," *Opt. Express* **22**(1), 96–101 (2014).
11. R. Takagi, R. Horisaki, and J. Tanida, "Object recognition through a multimode fiber," *Opt. Rev.* **24**(2), 117–120 (2017).
12. A. Porat, E. R. Andresen, H. Rigneault, D. Oron, S. Gigan, and O. Katz, "Widefield lensless imaging through a fiber bundle via speckle correlations," *Opt. Express* **24**(15), 16835–16855 (2016).
13. T. Čižmar and K. Dholakia, "Exploiting multimode waveguides for pure fibre-based imaging," *Nat. Commun.* **3**(1), 1027 (2012).
14. Y. Gong, W. Huang, Q. Liu, Y. Wu, Y. Rao, G. Peng, J. Lang, and K. Zhang, "Graded-index optical fiber tweezers with long manipulation length," *Opt. Express* **22**(21), 25267–25276 (2014).
15. E. E. Morales-Delgado, L. Urio, D. B. Conkey, N. Stasio, D. Psaltis, and C. Moser, "Three-dimensional microfabrication through a multimode optical fiber," *Opt. Express* **25**(6), 7031–7045 (2017).
16. N. Borhani, E. Kakkava, C. Moser, and D. Psaltis, "Learning to see through multimode fibers," *Optica* **5**(8), 960–966 (2018).
17. B. Redding, S. M. Popoff, and H. Cao, "All-fiber spectrometer based on speckle pattern reconstruction," *Opt. Express* **21**(5), 6584–6600 (2013).
18. H. Defienne, M. Barbieri, I. A. Walmsley, B. J. Smith, and S. Gigan, "Two-photon quantum walk in a multimode fiber," *Sci. Adv.* **2**(1), e1501054 (2016).
19. P. W. Brouwer, "Transmission through a many-channel random waveguide with absorption," *Phys. Rev. B* **57**(17), 10526–10536 (1998).

20. S. F. Liew, S. M. Popoff, A. P. Mosk, W. L. Vos, and H. Cao, "Transmission channels for light in absorbing random media: from diffusive to ballistic-like transport," *Phys. Rev. B* **89**(22), 224202 (2014).
21. M. Gong, Y. Yuan, C. Li, P. Yan, H. Zhang, and S. Liao, "Numerical modeling of transverse mode competition in strongly pumped multimode fiber lasers and amplifiers," *Opt. Express* **15**(6), 3236–3246 (2007).
22. M. Cheng, Y. Chang, A. Galvanauskas, P. Mamidipudi, R. Changkakoti, and P. Gatchell, "High-energy and high-peak-power nanosecond pulse generation with beam quality control in 200- $\mu\text{m}$  core highly multimode Yb-doped fiber amplifiers," *Opt. Lett.* **30**(4), 358–360 (2005).
23. F. Stutzki, F. Jansen, H.-J. Otto, C. Jauregui, J. Limpert, and A. Tünnermann, "Designing advanced very-large-mode-area fibers for power scaling of fiber-laser systems," *Optica* **1**(4), 233–242 (2014).
24. R. N. Mahalati, D. Askarov, and J. M. Kahn, "Adaptive modal gain equalization techniques in multimode Erbium doped fiber amplifiers," *J. Lightwave Technol.* **32**(11), 2133–2143 (2014).
25. R. Florentin, V. Kermene, J. Benoist, A. Desfarges-Berthelemot, D. Pagnoux, J.-P. Huignard, and A. Barthelemy, "Shaping the light amplified in a multimode fiber," *Light: Sci. Appl.* **6**(2), e16208 (2017) +supplementary.
26. S. M. Popoff, G. Lerosey, R. Carminati, M. Fink, A. C. Boccara, and S. Gigan, "Measuring the transmission matrix in optics: an approach to the study and control of light propagation in disordered media," *Phys. Rev. Lett.* **104**(10), 100601 (2010).
27. R. Florentin, V. Kermene, A. Desfarges-Berthelemot, and A. Barthelemy, "Fast transmission matrix measurement of a multimode optical fiber with common path reference," *IEEE Photonics J.* **10**(5), 1–6 (2018).
28. M. Plöschner, T. Tyc, and T. Čížmár, "Seeing through chaos in multimode fibres," *Nat. Photonics* **9**(8), 529–535 (2015).
29. A. Drémeau, A. Liutkus, D. Martina, O. Katz, C. Schülke, F. Krzakala, S. Gigan, and L. Daudet, "Reference-less measurement of the transmission matrix of a highly scattering material using a DMD and phase retrieval techniques," *Opt. Express* **23**(9), 11898–11911 (2015).
30. I. M. Vellekoop and A. P. Mosk, "Focusing coherent light through opaque strongly scattering media," *Opt. Lett.* **32**(16), 2309–2311 (2007).
31. A. Brignon and J.-P. Huignard, "Two-wave mixing in Nd:YAG by gain saturation," *Opt. Lett.* **18**(19), 1639–1641 (1993).
32. H. Chiang, J. Nilsson, J. Sahu, and J. R. Leger, "Experimental measurements of the origin of self-phasing in passively coupled fiber lasers," *Opt. Lett.* **40**(6), 962–965 (2015).